A red light-activable hetero-bimetallic [Fe(III)-Ru(II)] complex as a dual-modality PDT tool for anticancer therapy

Abhishek Panwar, Chandi C Malakar, Aarti Upadhyay*, and Mithun Roy*

Supporting Information

Table of Content

Materials and Methods

$[Fe(NO_3)_3.9H_2O]$, Bis(dichloro(η^6-p-cymene)ruthenium), bis(pyridin-2-ylmethyl)amine, bromoacetic acid, L-dopa, 1,10- phenanthroline-5-amine, (3-dimethylamino-propyl)-ethyl-carbodiimide (EDC.HCl), HOBt(1-Hydroxybenzotriazole), N, N-Diisopropylethylamine (DIPEA), sodium acetate, MTT, BSA, and sodium sulphate were procured from Sigma-Aldrich. Other chemicals and solvents were sourced from TCI Chemicals, Alfa-Aesar, SRL Chemical Company (India), and HI-MEDIA and were utilized without further purification. L-15 Media (Lonza), DMEM media (MP Biomedicals), Penicillin (Gibco), Streptomycin (Gibco), Fetal Bovine Serum (Gibco), Trypsin EDTA (Sigma-Aldrich), 6 well plates (Tarsons), Nunclon Sphera 3D Ultra-Low Attachment Microplate 96-well Clear Round Bottom (Thermo-Fisher Scientific), MTT Reagent (Invitrogen), Cell culture grade DMSO (MP Biomedicals). Other chemicals and solvents were purchased from TCI Chemicals, Alfa-Aesar, HI-MEDIA, and Finnar Chemicals and used without further purification. The solvents used were purified according to reported protocols prior to their use[1].

UV-visible spectra of the compounds and UV-visible spectroscopic experiments were performed using a Perkin-Elmer UV-visible spectrophotometer. The IR spectra were recorded using a Perkin-Elmer UATR Two FT-IR spectrophotometer. The Q-TOF-ESI mass spectra were recorded using Bruker Esquire 3000 and Agilent Accurate-Mass Q-TOF LC/MS 6546. Cyclic voltammetry studies were performed using Metrohm Autolab Potentiostat. The fluorescence spectra and fluorescence experiments were performed using a Hitachi F-7000 fluorescence spectrophotometer. For MTT, DCFDA, and Annexin-V/PI assays, one set of **[Fe-Ru]** treated cells was photoirradiated using a Waldmann PDT 1200 L (λ = 600−720 nm, light dose 30 J cm^{-2}). The cellular uptake of compounds was studied by fluorescence-activated cell sorting (FACS) analysis using BD FACS Verse Flow Cytometer. Annexin-V/PI assays were also performed on the same instrument. DCFDA assay was performed using a Leica SP8 Falcon microscope. Caspase-3/7 apoptosis was analyzed by utilizing the Caspase-Glo assay kit. To study intracellular localization of **[Fe-Ru]**, confocal laser scanning microscopy (CLSM) was done using a Zeiss LSM 880 with an Airyscan microscope containing an oil immersion lens having an amplification of 63×.

Hydroxyl radical generation study[2]

We measured the production of hydroxyl radicals by capturing them through the conversion of benzoic acid (0.2 mM) into salicylic acid using UV-visible spectrophotometry. The confirmation of hydroxyl radical production by the photo-Fenton degradation of [**Fe-Ru**] was achieved by adding a methanolic solution of $Fe(NO_3)_3.9H_2O$. The spectral signals of Fe(III)-salicylate, with a maximum wavelength (λ_{max}) of 520 nm, were seen to increase when exposed to red light (600-720 nm, 30 J/cm^{-2}) for 60 min in the presence of [**Fe-Ru**] (0.3 mM). The A_{520} of Fe(III)-salicylate showed a progressive rise, indicating the production of OH radicals.

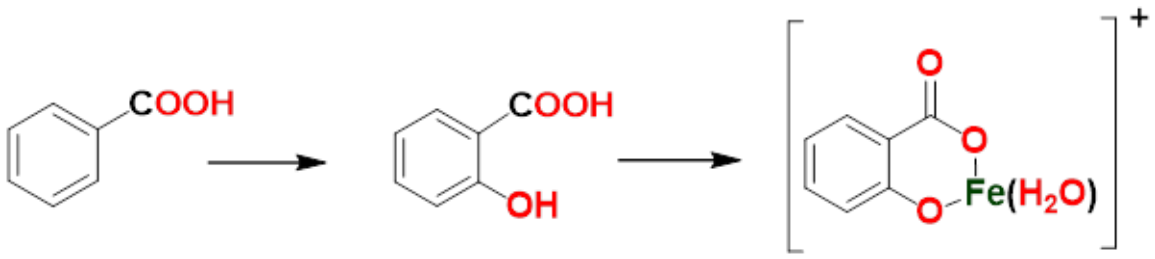

Singlet Oxygen ($^1O_2$) generation study[3]

DPBF experiment is used to detect singlet oxygen production. Initially, we measured the absorbance of DPBF using Rose Bengal. Then, we measure the absorbance of DPBF in the presence of the complex [**Fe-Ru**] (0.2 mM) without exposing it to light, which serves as the negative control. In this instance, the degree of $^1O_2$ production is measured by the absorbance (A_{417}) of DPBF decreasing to a certain level. To improve the graphical depiction, we have plotted the DPBF absorbance reduction extent (A_0-A/A_0) against the red light exposure duration (t/min), where A represents the DPBF absorbance at a certain time and A_0 represents the DPBF absorbance at t=0 min. We have seen a linear drop in DPBF absorbance with exposure duration, which suggests that type II photoprocessing is responsible for the photoinduced production of $^1O_2$ from $^3O_2$. To establish a correlation between the complex's photo-cytotoxicity and its singlet oxygen production during photoirradiation, the singlet oxygen quantum yield (ϕN) was further measured. It was found that the singlet oxygen quantum yield in DMSO ranged from 0.2 to 0.6, which was substantial for causing photocytotoxicity. The following formula was used to get the $^1O_2$ quantum yield.

$$\phi_N = \phi_{RB} \times \frac{K_N}{K_{RB}} \times \frac{A_{RB}}{A_N}$$

Where ϕN is the quantum yield of [**Fe-Ru**], K is the gradient of the decay rate constants of [**Fe-Ru**] and Rose Bengal, A is the light absorbed which is calculated from the integration of the absorption bands in the wavelength range from 400 to 700 nm.

Partition Coefficient Measurements[4,5]

Lipophilicity plays a vital role in influencing how medicine is distributed and how well it can permeate tissues. The partition coefficient was calculated by calculating the ratio of the complex concentration [**Fe-Ru**] in the octanol layer to its concentration in the aqueous layer ($P = c_{oct}/c_{water}$). The logP is the logarithm of the partition coefficient, which is the ratio of a substance's concentration in 1-octanol to its concentration in water. Deionized water was agitated with octanol for 24 h and thereafter subjected to centrifugation for 5 min to obtain water that was saturated with octanol, as well as octanol that was saturated with water. The complex [**Fe-Ru**] was dissolved in water that was saturated with octanol, at concentrations ranging from 0.03 to 3 mg mL^{-1}. The resulting solution was then combined with octanol that was saturated with water, in duplicate, using volumetric ratios of 1:1, 1:2, and 2:1. The mixtures were agitated using a vortexed for 0.5 h and subsequently separated by centrifugation for 5 min. The layers were methodically separated using a delicate gauge needle and subsequently examined for complex content by UV-visible spectroscopy.

BSA binding Studies[6]

Blood serves as the main carrier of pharmaceuticals in the human body, with the serum albumin protein playing a crucial role in transporting the drugs to their intended target. An experiment was carried out to analyze protein binding using tryptophan fluorescence quenching studies. A stock solution of bovine serum albumin (BSA) was prepared with a concentration of 3 X 10^{-5} M, calculated based on its molecular mass of 66000 Da. The tests were conducted using a 10 mM Tris-HCl buffer solution with a pH of 7.2 to preserve circumstances that are similar to those seen in living organisms. The emission intensity of tryptophan residues of BSA at ~348 nm was monitored to observe the quenching effect caused by the complex [**Fe-Ru**] (0.003 mM), as its concentration was increased. Fluorescence measurements were conducted at room temperature using a HITACHI F-7000 fluorescence spectrophotometer. The concentration of BSA was maintained at a constant value of 2 mL, with a molar concentration of 3 X 10^{-5} M. The concentration of the quencher was varied during the experiment. The data was subjected to a linear regression analysis using the Stern-Volmer equation.

$$\frac{I_0}{I} = +kq\tau_0[Q] = 1 + K_{sv}[Q]$$

Cell culture conditions

The Human alveolar basal epithelial (A549) cell lines, Henrietta Lacks cell line (HeLa), and human peripheral lung epithelial (HPL1D) cells were purchased from the American Type Culture Collection (ATCC). The cells were in L-15 Media, the cells were maintained in DMEM media supplemented with penicillin (100 units mL^{-1}), streptomycin (100 mg mL^{-1}), and 10% Fetal Bovine Serum (FBS) and incubated at 37°C in a humidified, 5% CO_2 atmosphere. The cells were passaged using 0.25% Trypsin-EDTA solution. All experiments were performed using passage numbers between 38 – 42.

Cytotoxicity assay (MTT assay)[7-8]

The cytotoxicity of the [**Fe-Ru**] complex was investigated by MTT assays. Adenocarcinomic human alveolar basal epithelial cell line (A549), Henrietta Lacks cell line (HeLa), was cultured in DMEM media supplemented with 10% FBS. The cells were maintained at 37 °C in a humidified atmosphere with 5% CO_2. Approximately, 5000 cells were plated in each well of four 96-well tissue culture plates. The cells were treated with **Fe, Ru,** and [**Fe-Ru**] complex in the range of 1μM to 100 μM different concentrations in 1% DMSO/Dulbecco's modified Eagle's medium (DMEM) with each having two sets of 96-well tissue culture plates. One set of the cells was exposed to red light (15-minute exposure, λ = 600-720 nm, light dose = 30 J cm^{-2}) in DPBS (Dulbecco's phosphate-buffered saline) using a Waldmann PDT 1200 L whereas the other set was kept in the dark for the same period. After exposure to light, DPBS was removed and replaced with fresh medium and the cells were kept at 37 °C for a further period of 19 h. The DPBS buffer containing 3-(4,5-dimethylthiazol-2-yl)-2,5- diphenyltetrazolium bromide (MTT, 20 μL of 5 mg mL^{-1}) was then added into each well and incubated for 4 h. The medium was then discarded, DMSO (200 μL) was added to dissolve the purple formazan crystals, and the absorbance was recorded at 570 nm for each well using a TECAN microplate reader, and graphs were plotted by using GraphPad Prism 7 software. Data were obtained by using three independent sets of experiments done in triplicate for each concentration.

Cell imaging study[9]

For imaging study, the adenocarcinoma human alveolar basal epithelial cell line (A549) cells were plated in treated 35 mm Ibidi Corning dishes at a seeding density of 0.60×10^5 cells per dish and allowed to grow to confluence (48 h). The dishes were aspirated and cells were treated with complex [**Fe-Ru**] (2.5 μM), suspended in a mixture of PBS and media (without FBS). The cells were further incubated from time to time for 1h, 2h, and 3h at 37 °C in a humidified atmosphere of 5% CO_2 in air. Finally, the cells were washed twice with PBS buffer and placed in PBS with Trypan blue for imaging studies.

DCFDA assay[10]

Cellular reactive oxygen species (ROS) was detected by 7'-dichlorofluorescein diacetate (DCFDA) assay. Cellular ROS oxidizes cell permeable DCFDA generating a fluorescent DCF having emission maxima at 528 nm. The percentage population of cells generating ROS was determined by Flow Cytometry analysis. A549 cells were incubated with the compounds at their IC_{50} value of 1.4 μM for 4 h and then irradiated with red light for 15 min (λ = 600-720 nm, light dose = 30 J cm^{-2}) using Waldmann PDT 1200 L. The cells were harvested by trypsinization and a single-cell suspension was prepared. The cells were subsequently treated with 1 μM DCFDA (solution prepared with DMSO) in the dark for 20 min at room temperature. The distribution of DCFDA-stained A549 cells was obtained by flow cytometry in the FL-1 channel.

Cellular Uptake Studies[4]

The adenocarcinoma human alveolar basal epithelial cell line (A549) cells were on glass coverslips in 12 well tissue culture plates and incubated at 37 °C and 5% CO_2 atmosphere for 24 h. Then the cells were incubated with [**Fe-Ru**] (2.5μM) at 37 °C for 4 h. The cells were then washed once with chilled phosphate buffer saline and analyzed by Flow Cytometry on an FL2 channel.

Annexin-V/FITC Assay[10]

About 4 x 10^5 A549 cells were plated in 96 well plates and grown for 24 h and cells were treated with the [**Fe-Ru**] complex (2.5 μM) for 4 h. One of the plates was exposed to photo-irradiation (600-720 nm, 30 Jcm^{-2}, 15 min) in DPBS followed by the addition of fresh media. The cells were further incubated for 1 h, trypsinized, and washed in DPBS twice. The cells were then re-suspended in 400 μL of 1X binding buffer and 1 μL of annexin V-FITC and 2 μL of PI were added to each cell suspension. These tubes were then incubated at room temperature for 20 min in the dark and the fluorescence of the cells was measured immediately with a flow cytometer. Cells that are early in the apoptotic process were stained with the annexin V-FITC alone while live cells showed no staining by either PI or annexin V-FITC. Late apoptotic cells were stained by both PI and annexin V-FITC while the dead cells were only stained by PI.

Caspase 3/7 activation assay [11]

A549 cells were seeded in white-walled nontransparent-bottomed 96-well microculture plates at a density of 4 × 10^5 cells/well and allowed to incubated overnight to adhere. The cells were then treated with culture medium (negative control, NC), 1% DMSO culture medium (DMSO), 10 μM cisplatin (cis-Pt) or 2.5 μM [**Fe-Ru**] complex, respectively. The cells were incubated for 4 h in the dark and divided into two equal parts. The dark group was incubated for additional 30 min and treated with Caspase-Glo 3/7 activity kit according to the manufacturer's protocol, and the luminescence in RLUs was quantified by an Infinite M200 PRO (TECAN, Swiss). The other groups were exposed to red light irradiation (600–720 nm, 30 J cm^{-2}), and incubated for additional 30 min in the dark. The caspase-3/7 activity was measured by identical method.

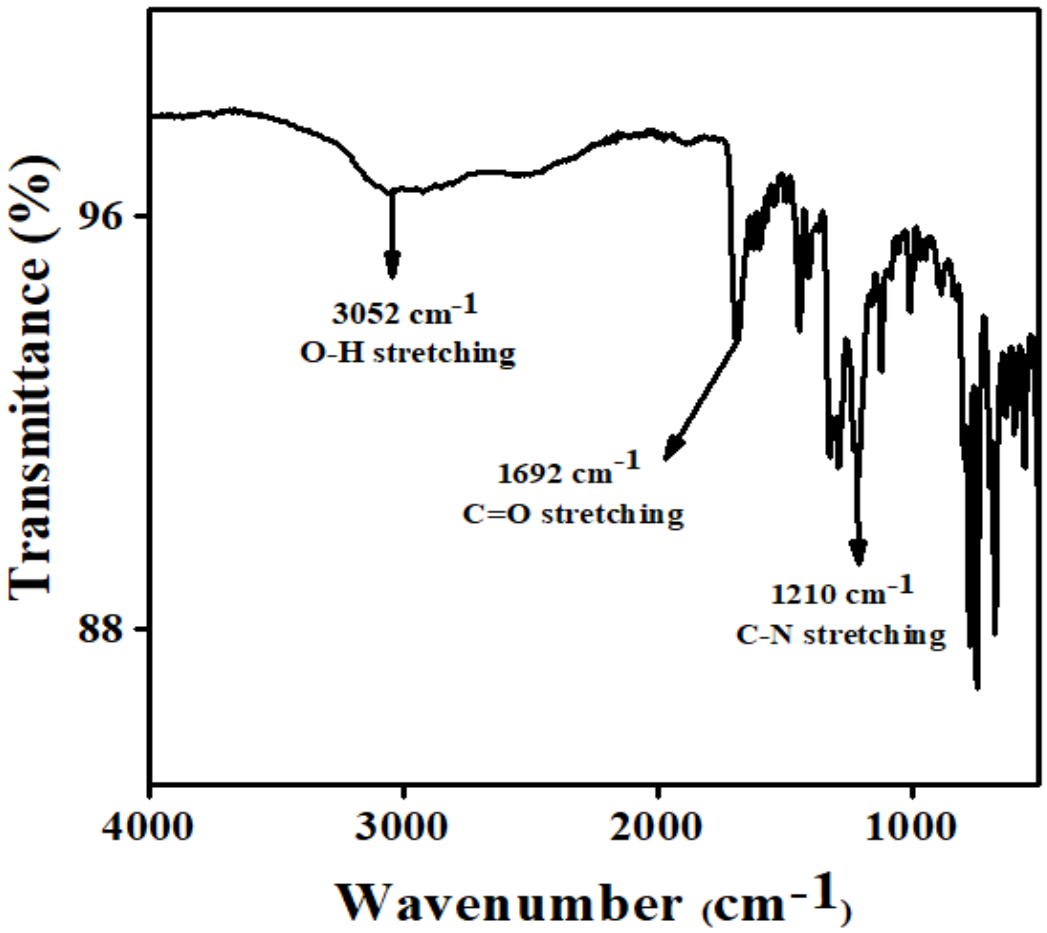

Figure S1. FT-IR Spectra of **L**[1] complex recorded in KBr phase using Perkin-Elmer UATR TWO FT-IR Spectrometer.

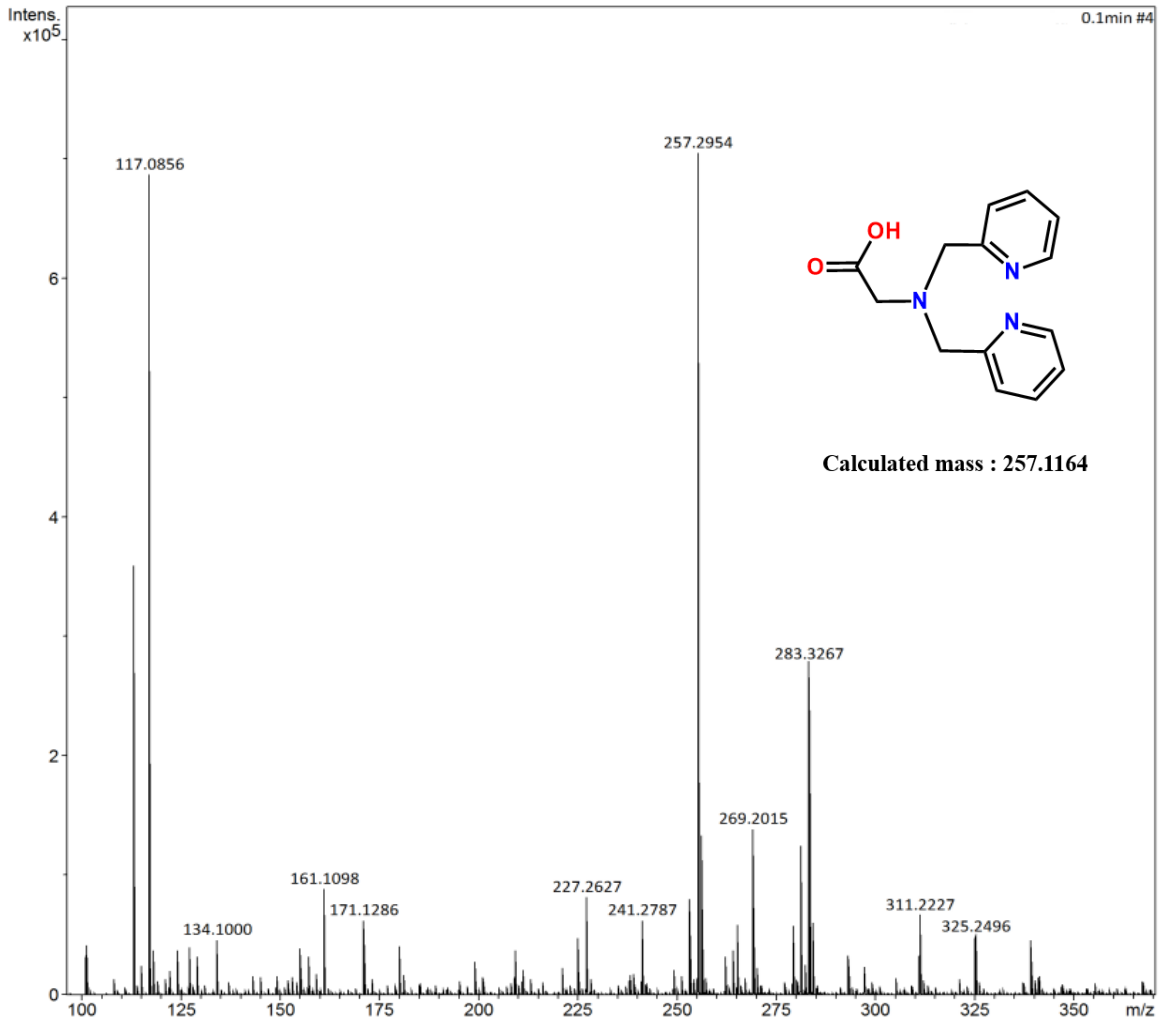

Figure S2. Q-TOF ESI Mass spectra of the $\mathbf{L^1}$ was recorded in CH_3OH using Bruker Esquire 3000 Plus spectro-photometer (Bruker-Franzen Analytic GmbH, Bremen, Germany). The peak at m/z is 257.2954, which corresponds to the species $[\mathbf{L^1}]^{\cdot+}$.

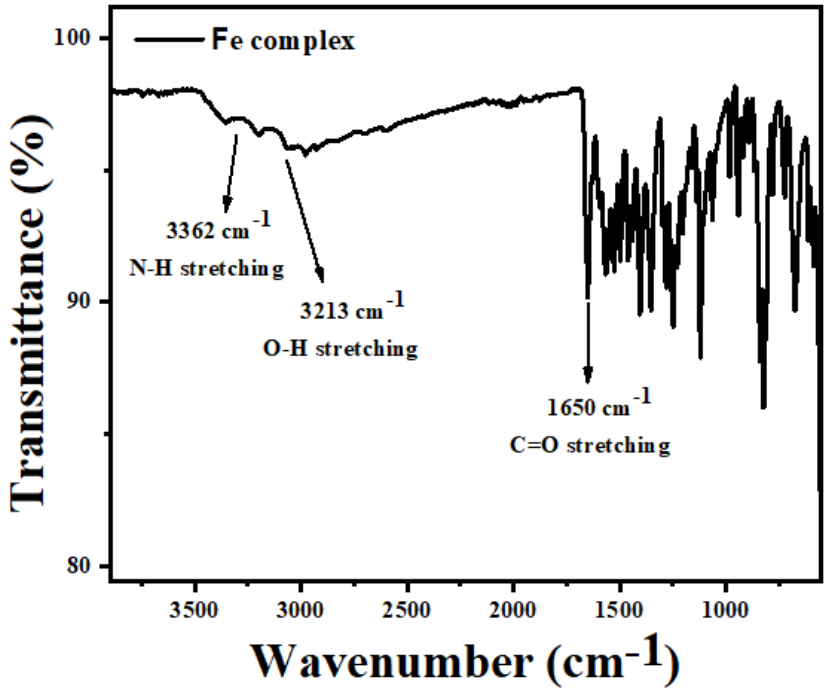

Figure S3. FT-IR Spectra of **Fe** complex recorded in KBr phase using Perkin-Elmer UATR TWO FT-IR Spectrometer.

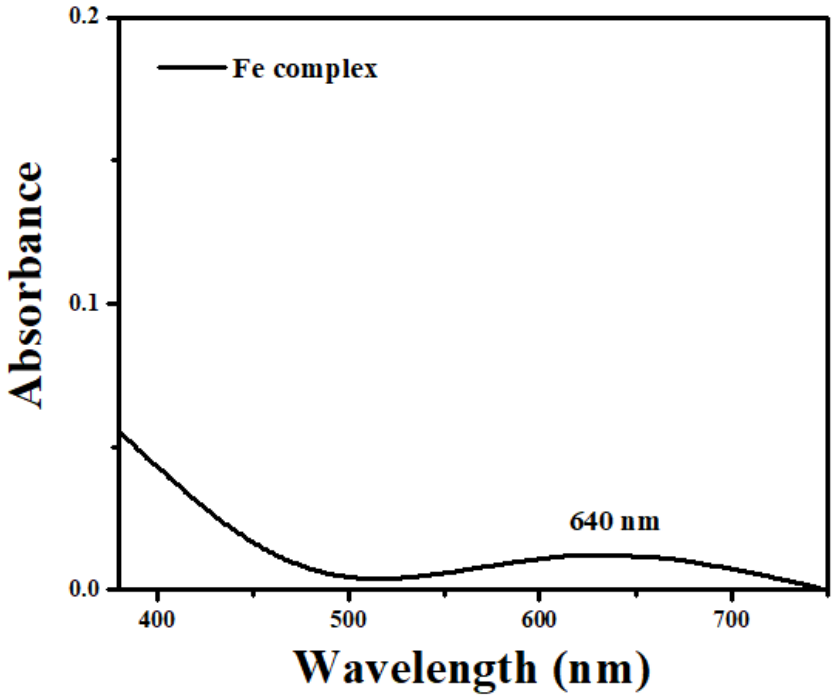

Figure S4. UV-visible spectra of **Fe** complex (0.02 mM) in 5% DMSO-PBS buffer at pH 7.4 in 298 K.

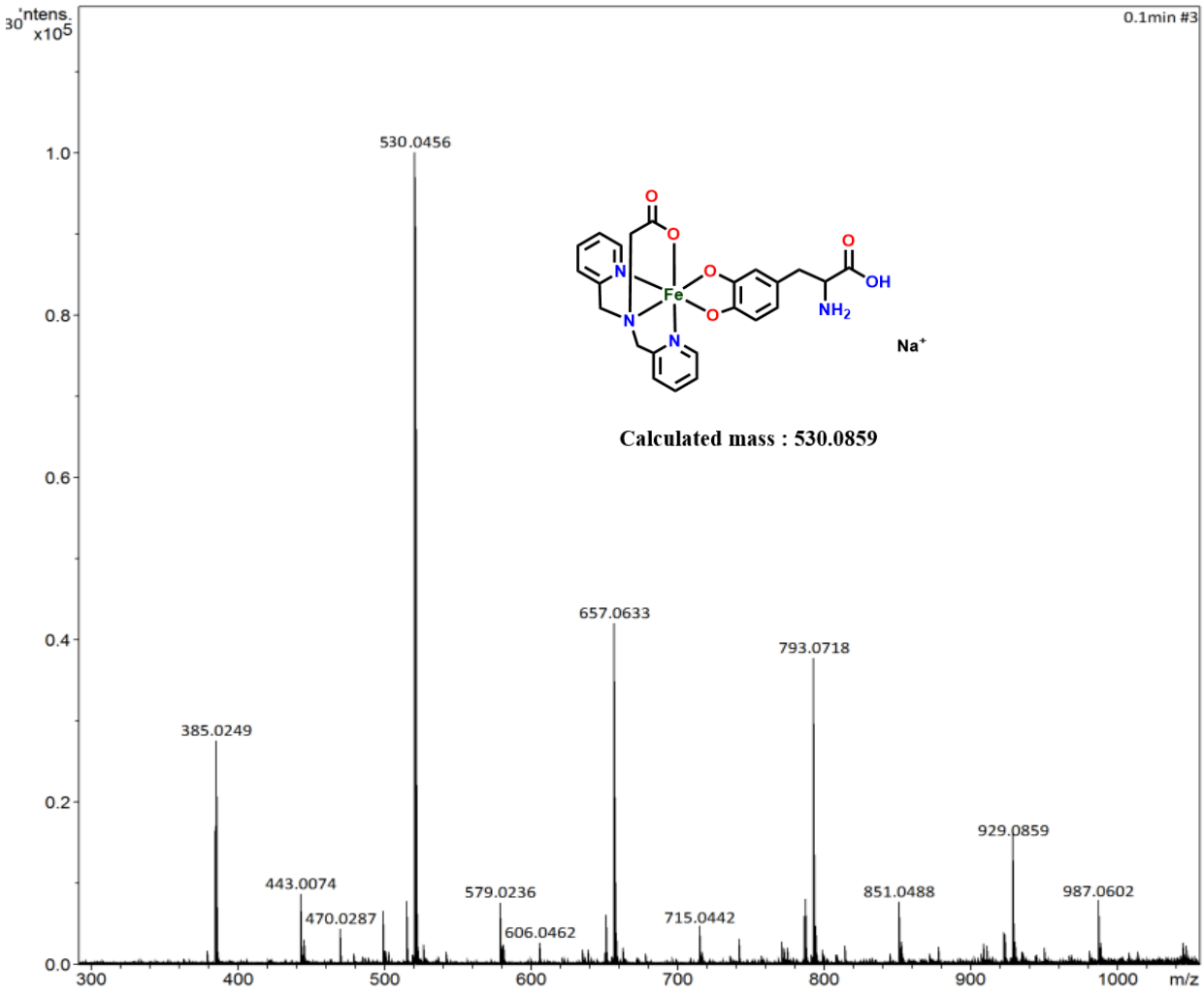

Figure S5. Q-TOF ESI Mass spectra of the **Fe** complex was recorded in DMF using Bruker Esquire 3000 Plus spectro-photometer (Bruker-Franzen Analytic GmbH, Bremen, Germany). The peak at m/z is 530.0456, which corresponds to the species [**Fe**-Na]$^{+}$.

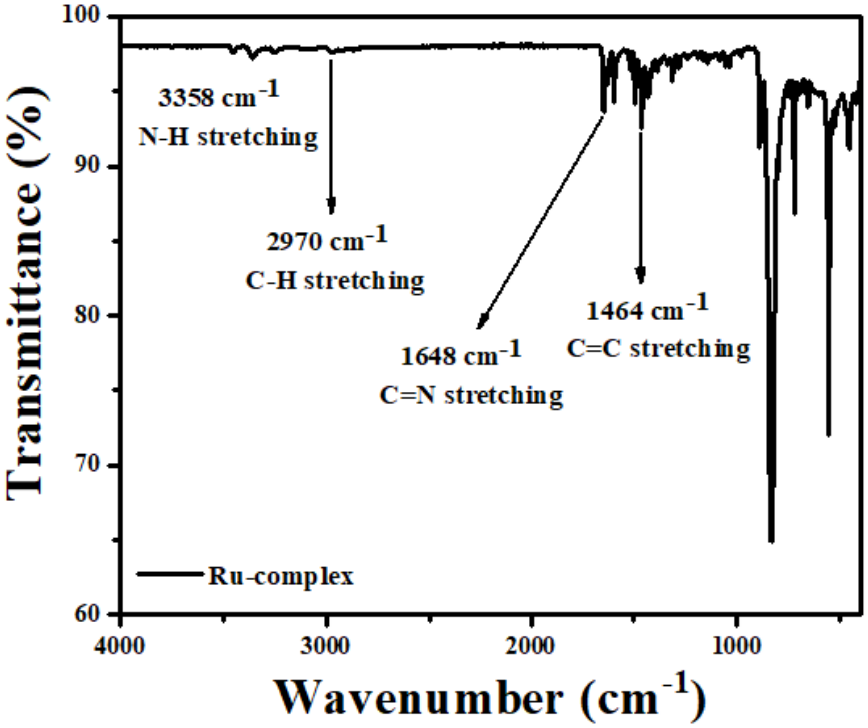

Figure S6. FT-IR Spectra of **Ru** complex recorded in KBr phase using Perkin-Elmer UATR TWO FT-IR Spectrometer.

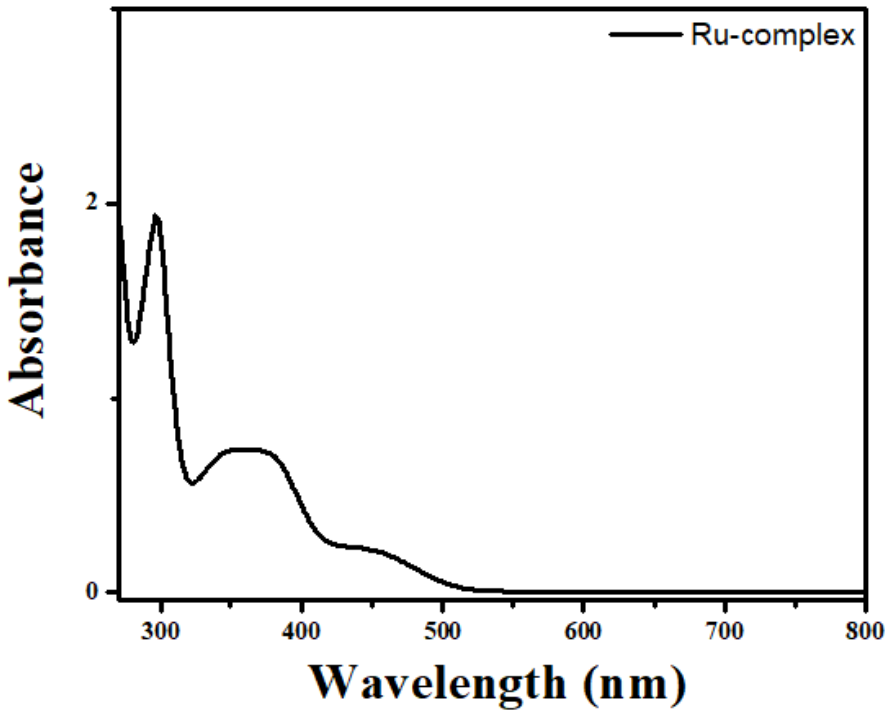

Figure S7. UV-visible spectra of **Ru** complex (0.1 mM) in 5% DMSO-PBS buffer at pH 7.4 in 298 K.

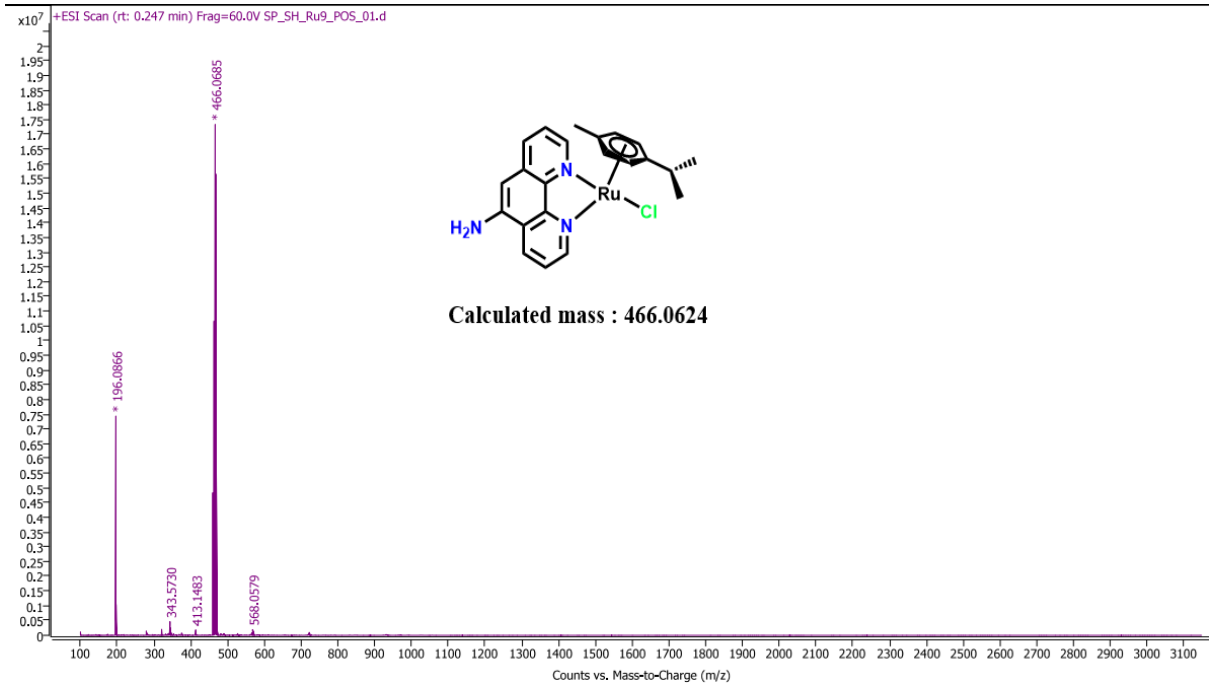

Figure S8. Q-TOF ESI Mass spectra of the **Ru** complex recorded in CH_3OH an Agilent Accurate-Mass Q-TOF LC/MS 6546. The peak at m/z 466.0685 corresponds to the species $[\mathbf{Ru}]^{\cdot+}$.

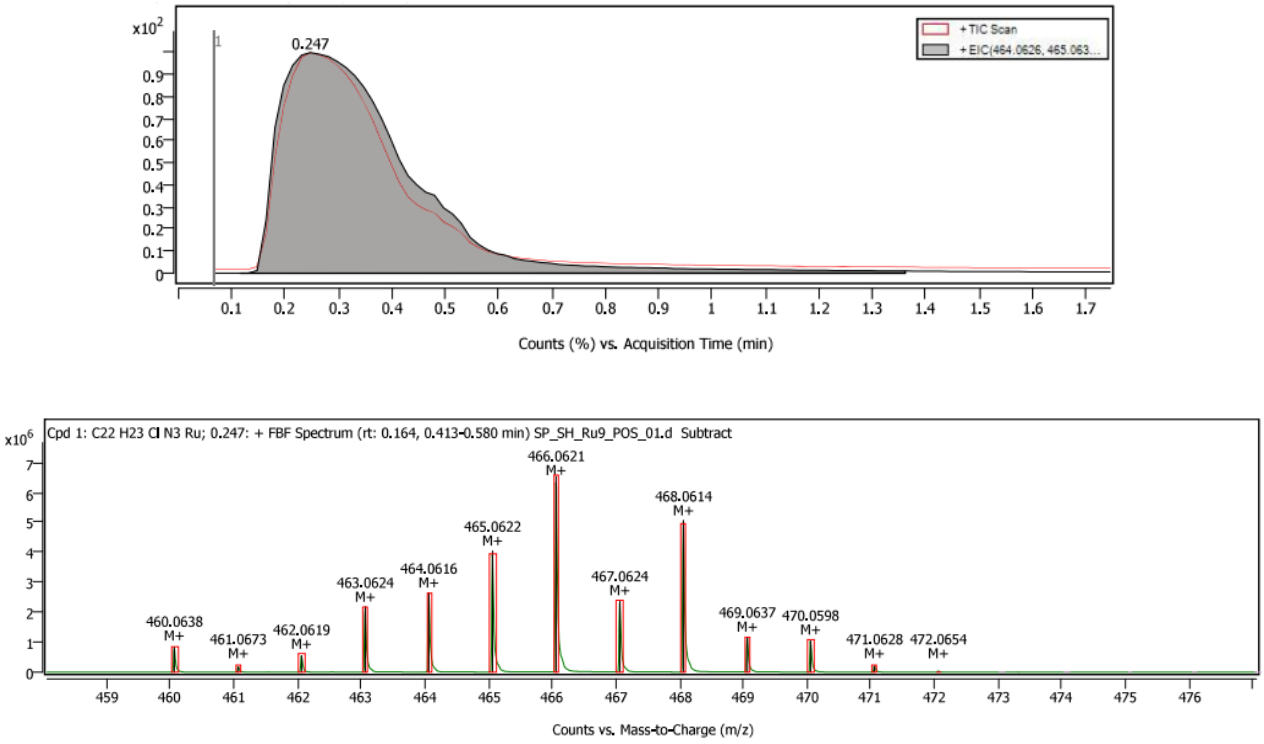

Figure S9. Simulated isotopic distribution mass spectra of the **Ru** complex recorded in CH_3OH using an Agilent Accurate-Mass Q-TOF LC/MS 6546. The peak at m/z 466.0621 corresponds to the species $[\mathbf{Ru}]^{\cdot+}$.

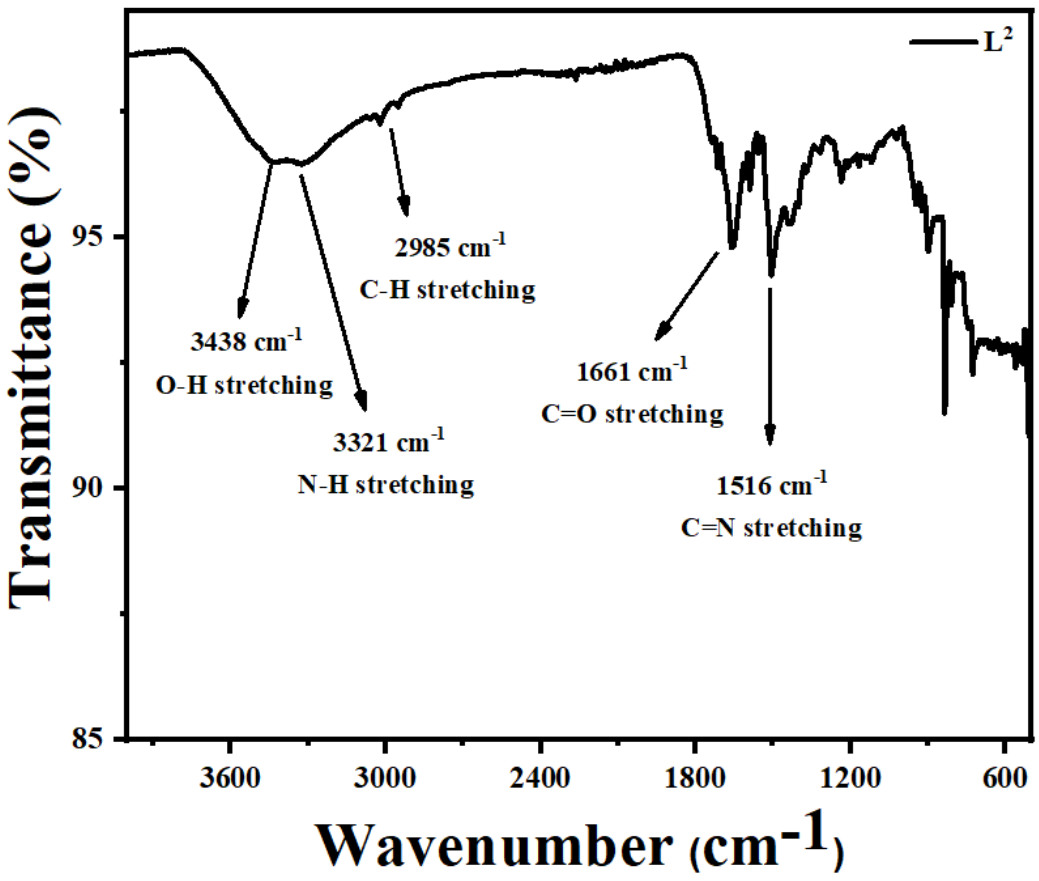

Figure S10. FT-IR Spectra of **L^2** ([L-dopa(COO-NH_2)phen]) recorded in KBr phase using Perkin-Elmer UATR TWO FT-IR Spectrometer.

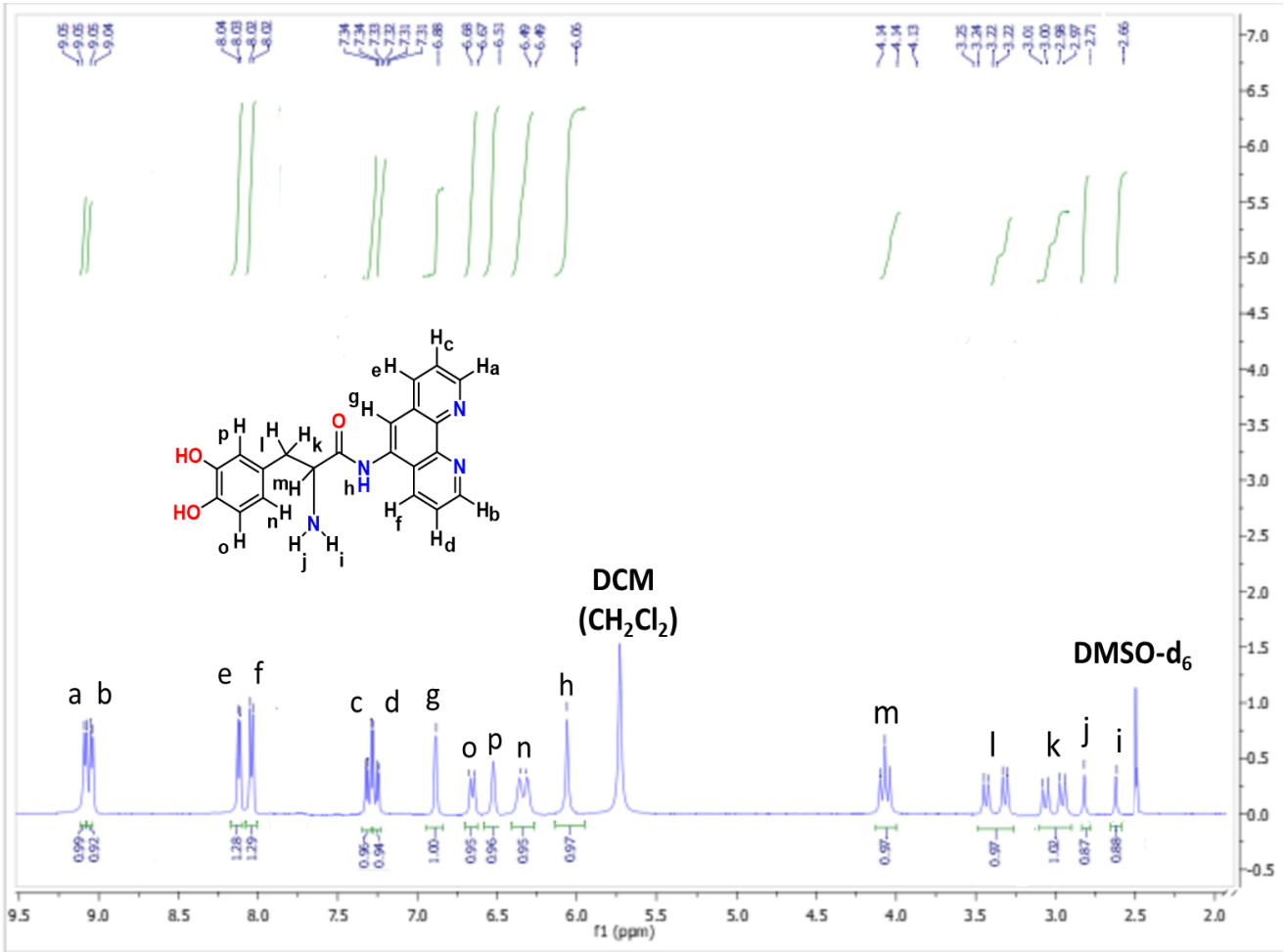

Figure S11. ^{1}H NMR of (**L^{2}**) [L-dopa(COO-NH_2)phen] recorded in DMSO-d_6 using Bruker Avance 400 (500 MHz) spectrometer (DMSO-d_6 = 2.5 ppm).

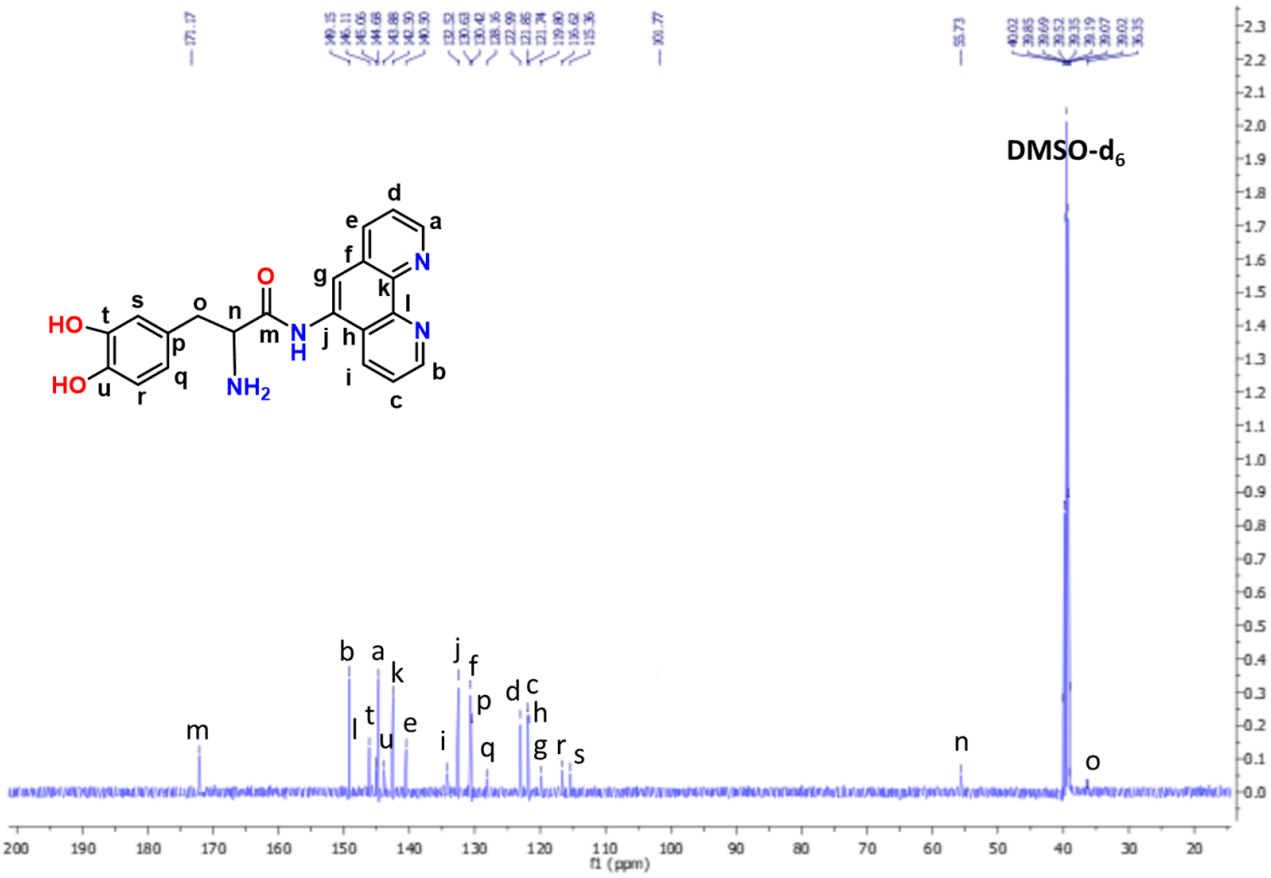

Figure S12. ^{13}C NMR of (**L^2**) [L-dopa(COO-NH_2)phen] recorded in DMSO-d_6 using Bruker Avance 400 (126 MHz) spectrometer (DMSO-d_6 = 39.52 ppm).

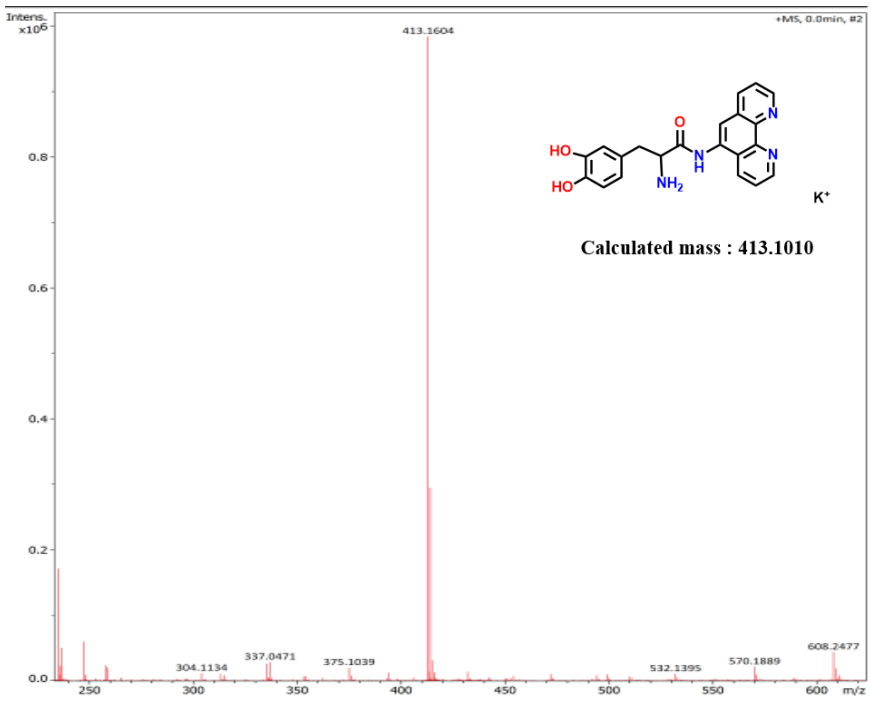

Figure S13. Q-TOF ESI Mass spectra of the **L²** complex was recorded in methanol using Bruker Esquire 3000 Plus spectro-photometer (Bruker-Franzen Analytic GmbH, Bremen, Germany). The peak at m/z is 413.1604, which corresponds to the species $[\mathbf{L}^2+K]^+$.

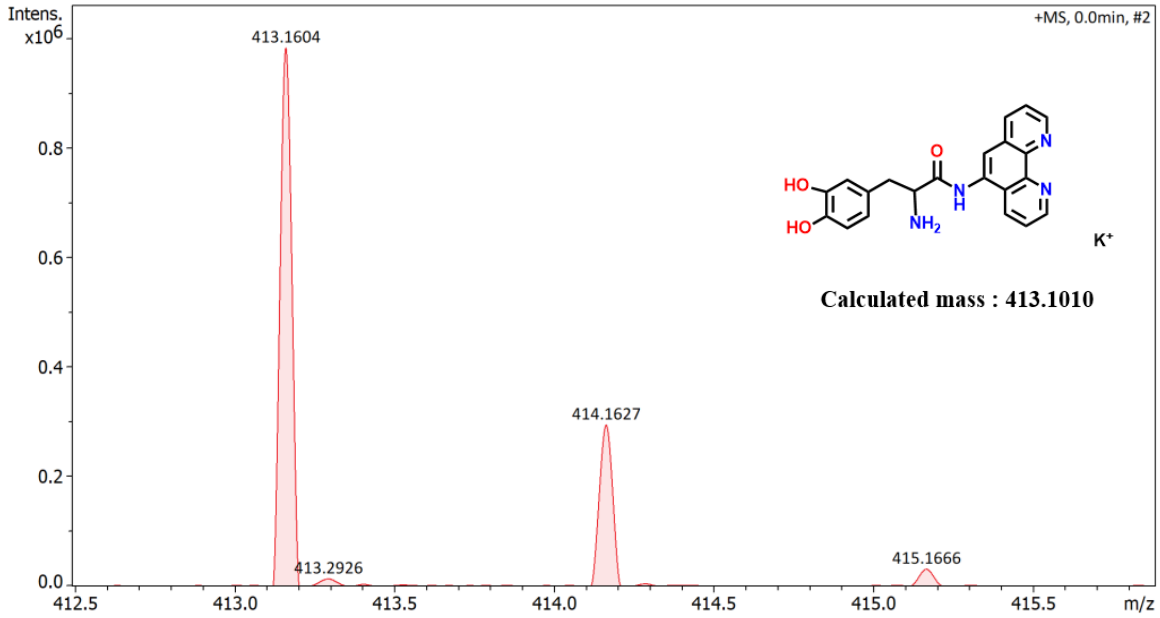

Figure S14. Simulated isotopic distribution mass spectra of the **L²** recorded in CH_3OH using Bruker Esquire 3000 Plus Spectro-photometer (Bruker-Franzen Analytic GmbH, Bremen, Germany). The peak at m/z 413.1604 corresponds to the species $[\mathbf{L}^2+K]^+$.

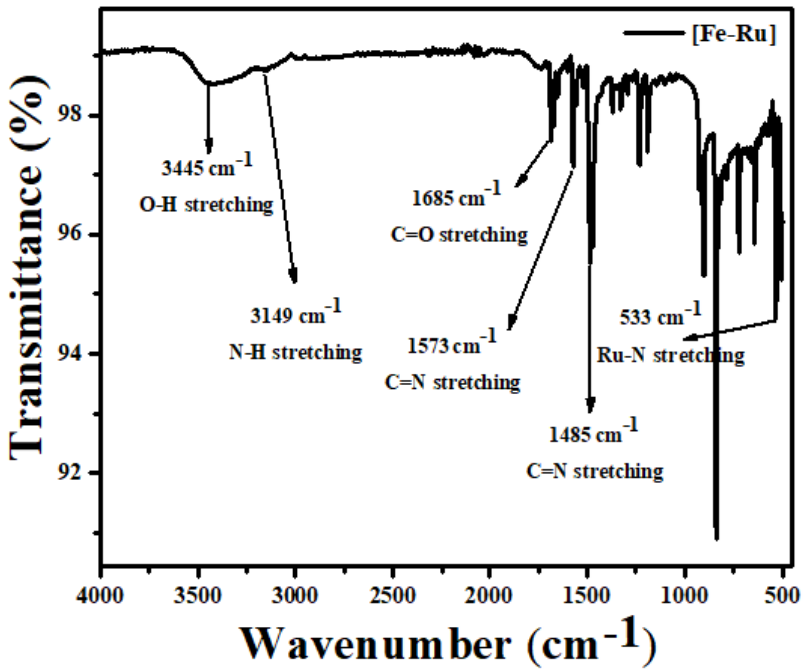

Figure S15. FT-IR Spectra of **[Fe-Ru]** complex recorded in KBr phase using Perkin-Elmer UATR TWO FT-IR Spectrometer.

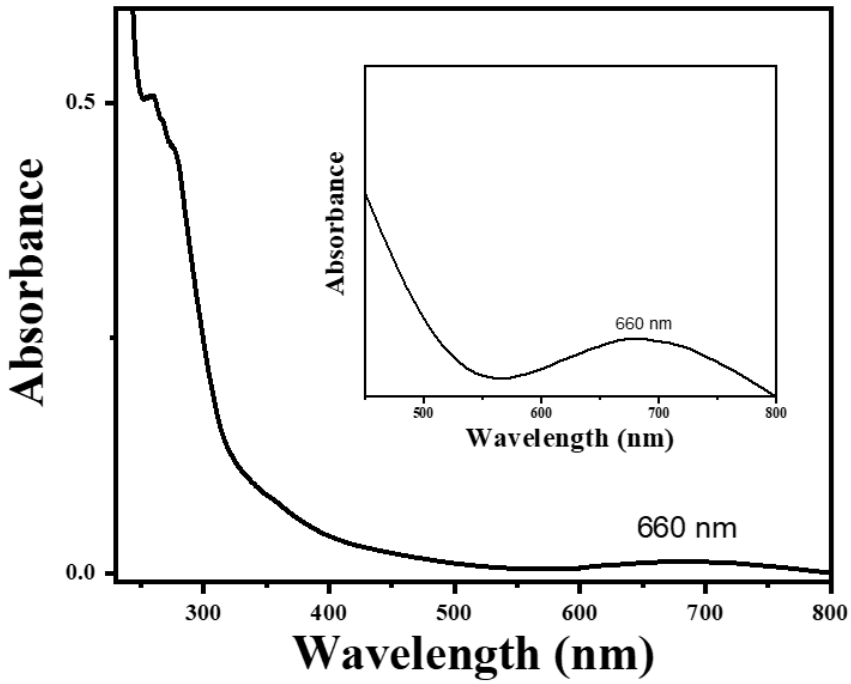

Figure S16. UV-visible spectra of [**Fe-Ru**] complex (0.02 mM) in 5% DMSO-PBS buffer at pH 7.4 in 298 K.

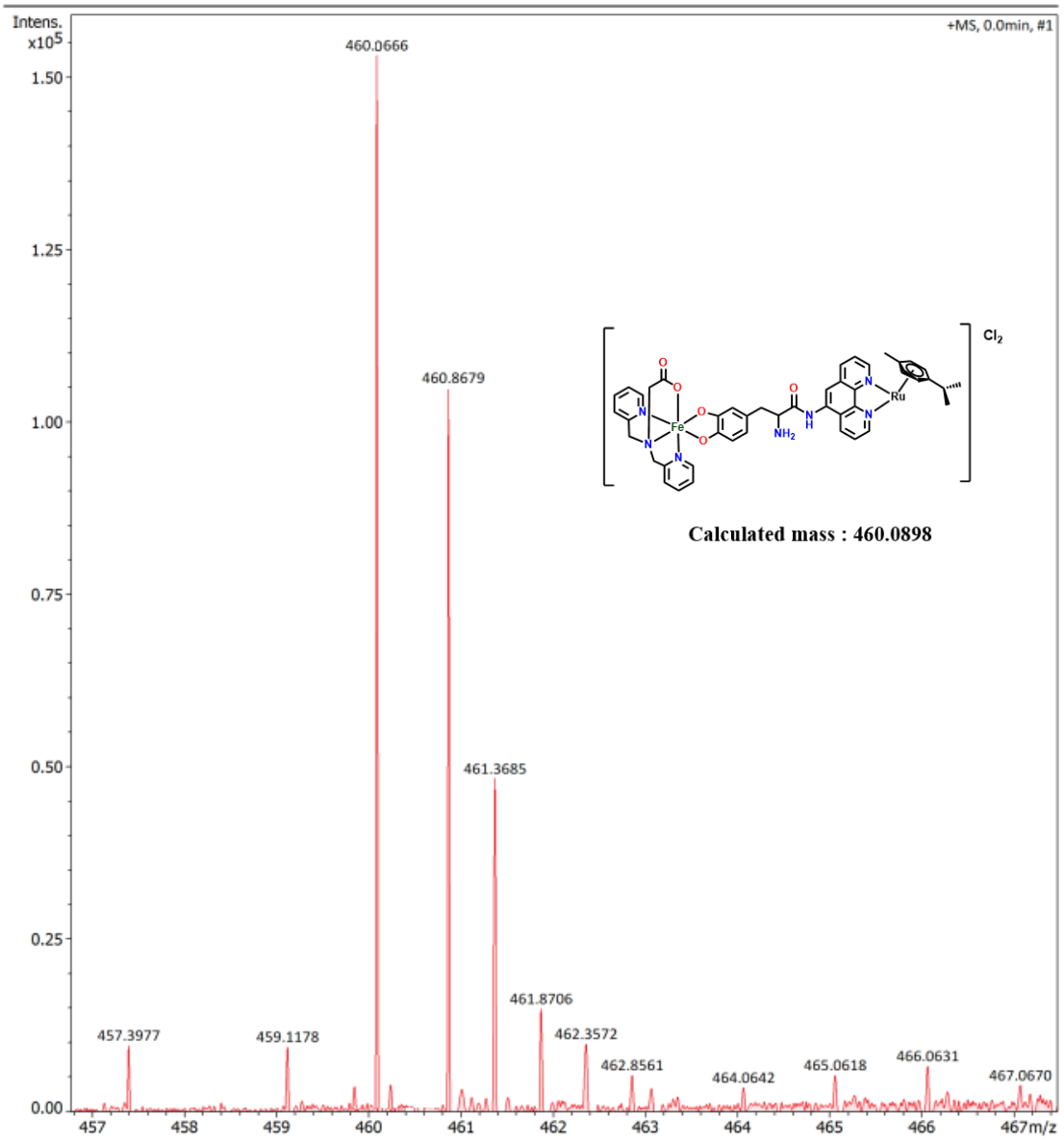

Figure S17. Simulated isotopic distribution fragmented mass spectra of the **[Fe-Ru]**$^{+2}$ recorded in CH_3OH using Bruker Esquire 3000 Plus Spectro-photometer (Bruker-Franzen Analytic GmbH, Bremen, Germany). The peak at m/z 460.0666 corresponds to the general formula $[M\text{-}Cl]^{2+}$, where M represents [**Fe-Ru**].

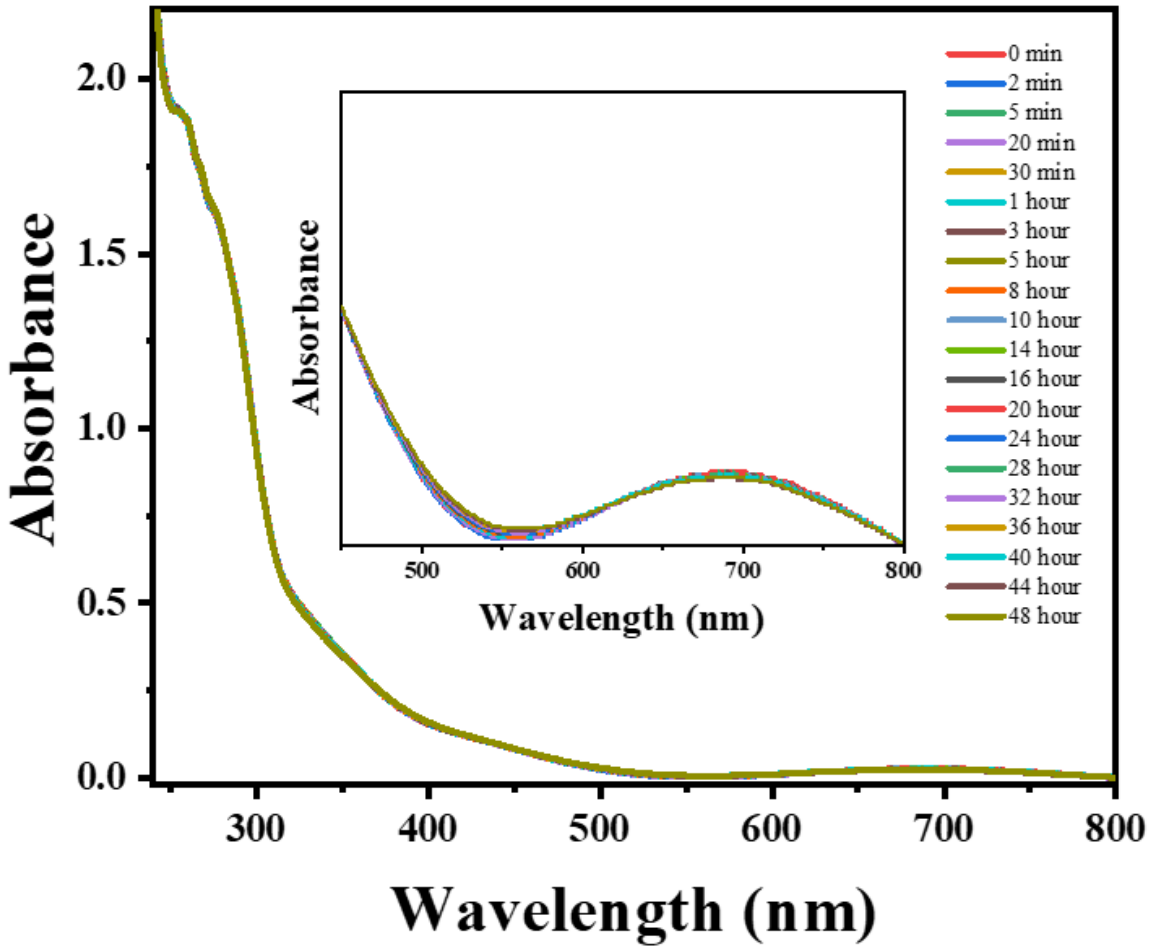

Figure S18. Stability of **[Fe-Ru]** (0.02 mM) in a 5 % DMSO-PBS buffer medium at pH = 7.4 and room temperature in the dark for up to 48 h.

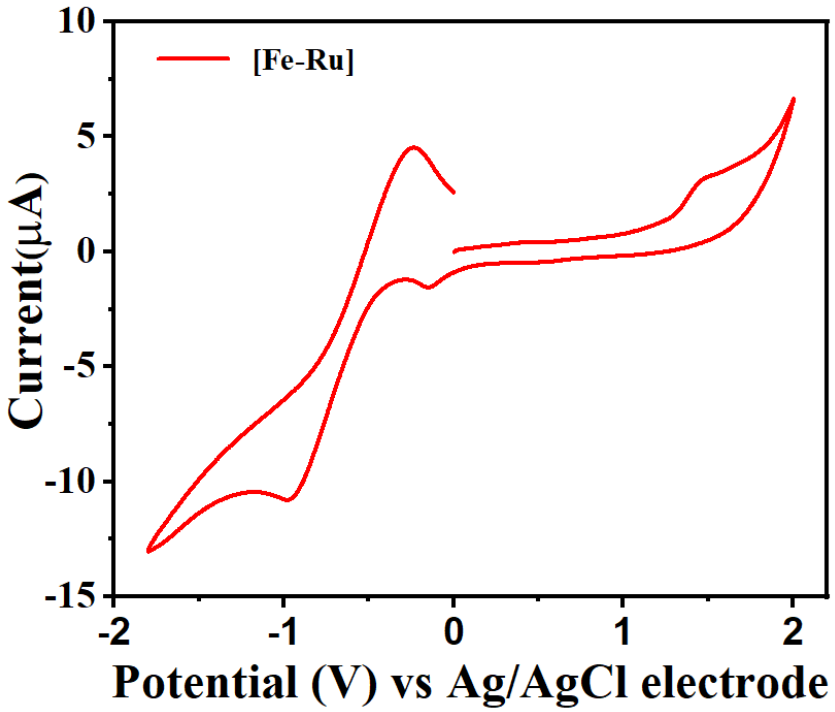

Figure S19. Cyclic Voltammogram (full scan) of [**Fe-Ru**] complex (0.03 mM) in a 5% DMSO-PBS buffer solution at room temperature at dark, using Glassy Carbon electrode as working electrode, Ag/AgCl electrode as reference electrode and Pt electrode as counter electrode and 0.1 M KCl as supporting electrolyte, at a scan rate 50 mV/s.

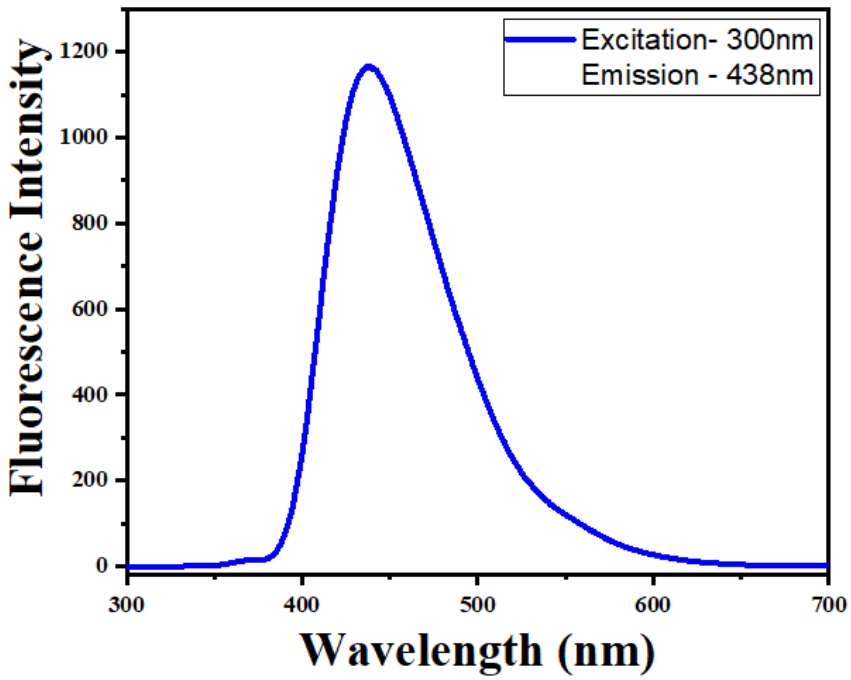

Figure S20. Emission spectra of **[Fe-Mn]** complex (0.03 mM) in a 5% DMSO-PBS buffer medium at pH 7.4 and room temperature, λ_{ex}: 300 nm.

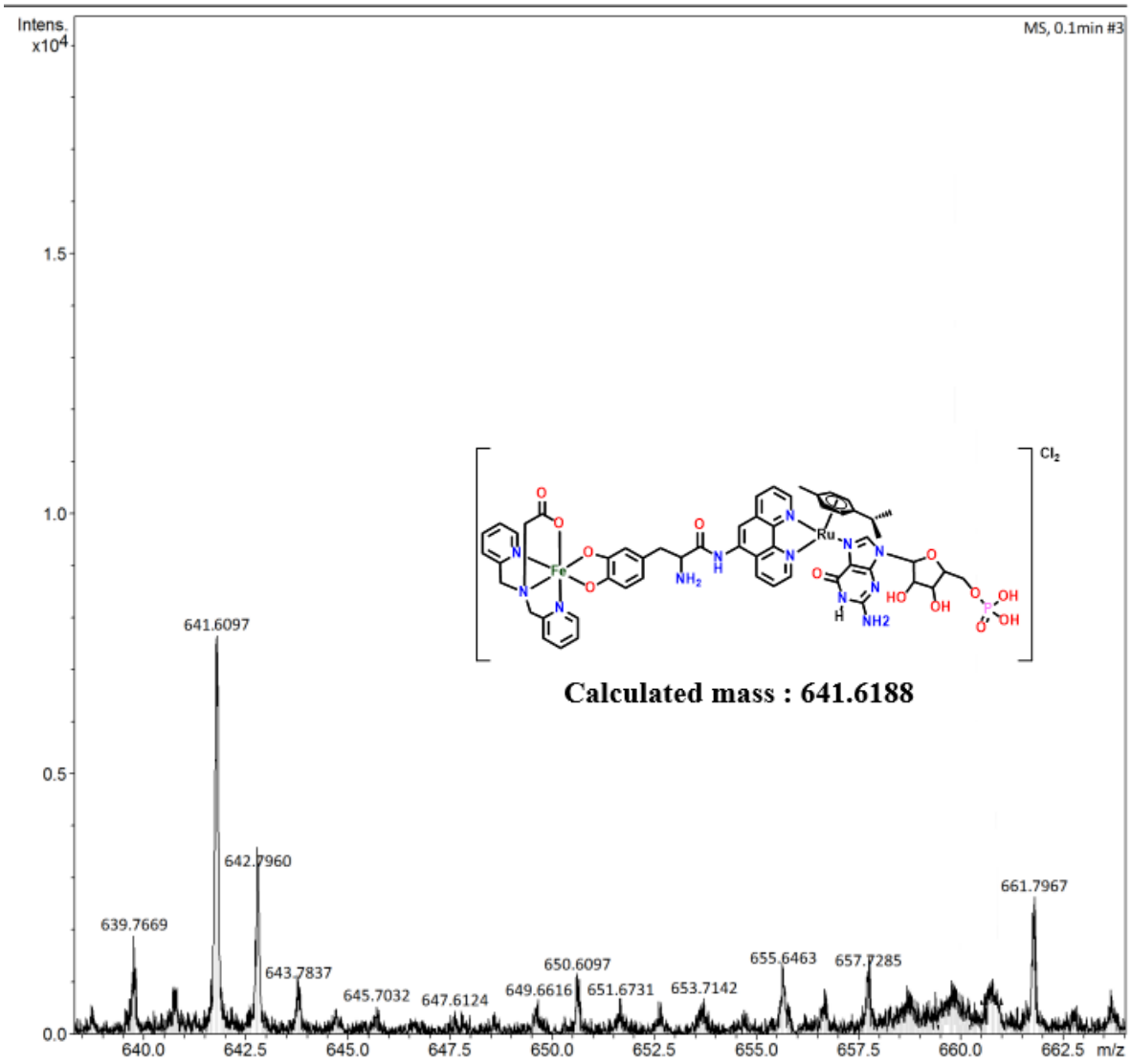

Figure S21. Simulated isotopic distribution mass spectra of the **[Fe-Ru-N^7-GMP]**$^{+2}$ recorded in DMF using Bruker Esquire 3000 Plus Spectro-photometer (Bruker-Franzen Analytic GmbH, Bremen, Germany). The peak at m/z 641.6097 corresponds to the general formula [M-Cl]$^{+2}$, where M represents [**Fe-Ru**-N^7-GMP].

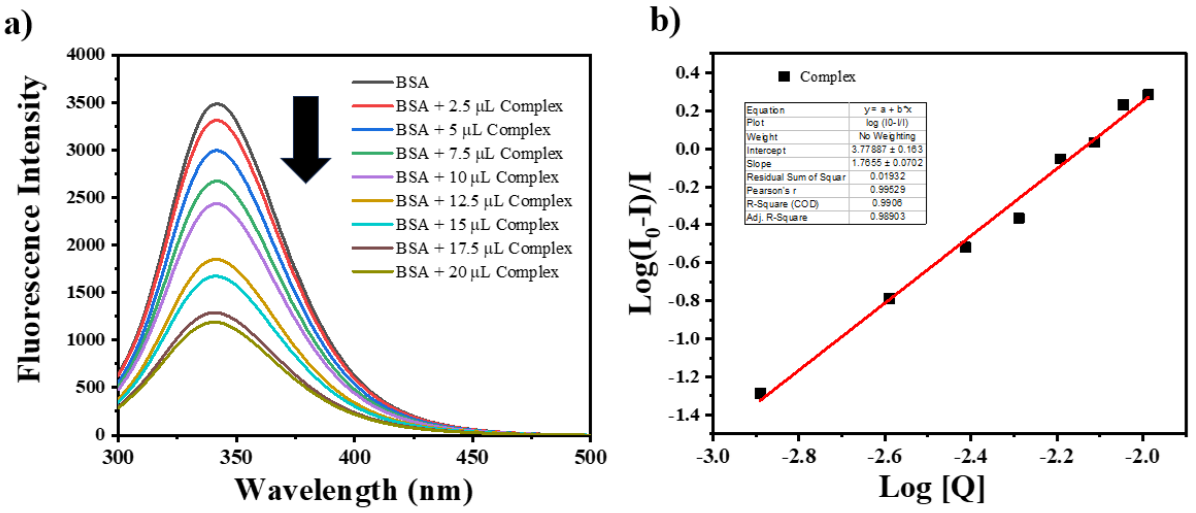

Figure S22. a) BSA binding studies of **[Fe-Ru]** complex (0.3 mM) taking 200 µL BSA from (3×10^{-5}) M stock in Tris-HCl-Buffer (5 mM, pH = 7.2) at room temperature, a Scatchard plot (b) is being added.

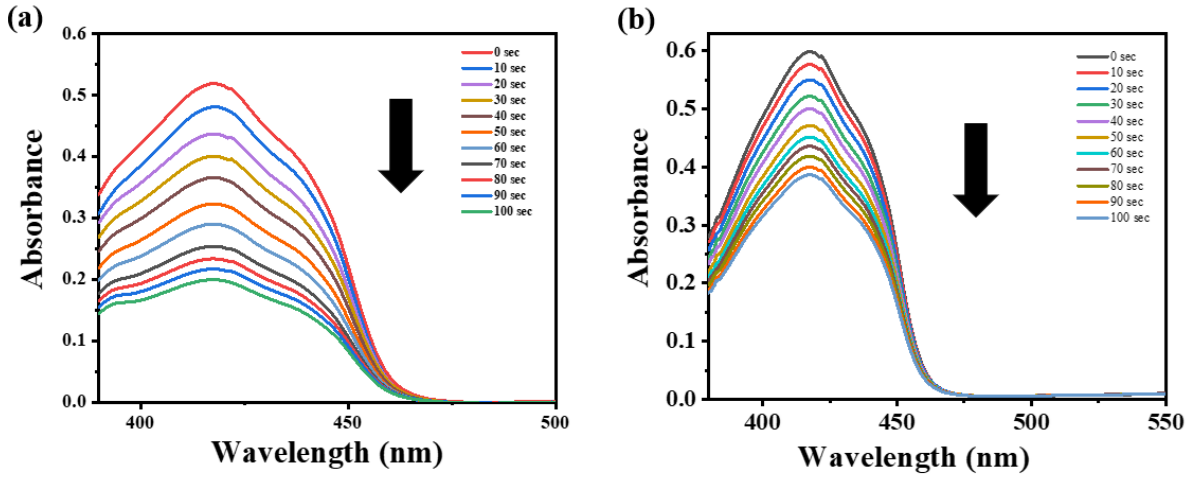

Figure S23. Spectroscopic studies on the generation of singlet oxygen by a) [**Fe-Ru**] complex (0.2 mM) and b) Ruthenium-paracymene-phenanthroline complex (**Ru**) (0.2 mM) upon photo-activation in red light (30-Watt, 600-720 nm) in DMSO at 298 K.

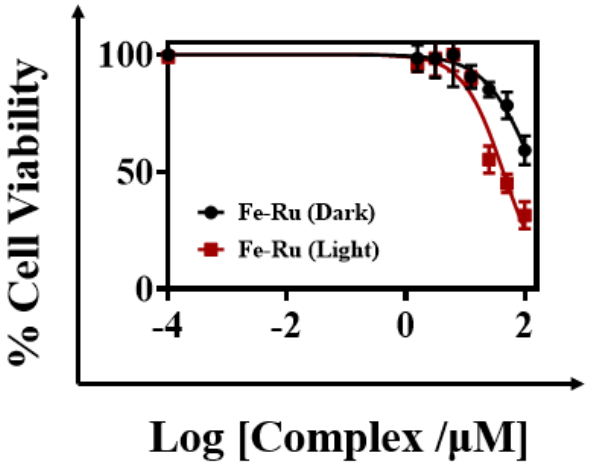

Figure S24. Cell viability (MTT assay) plots showing the cytotoxicity of **[Fe-Ru]** complex in HPL1D cells in the dark (black symbols) and in the presence of red light (red symbols, 600-720 nm, 30 J cm^{-2}).

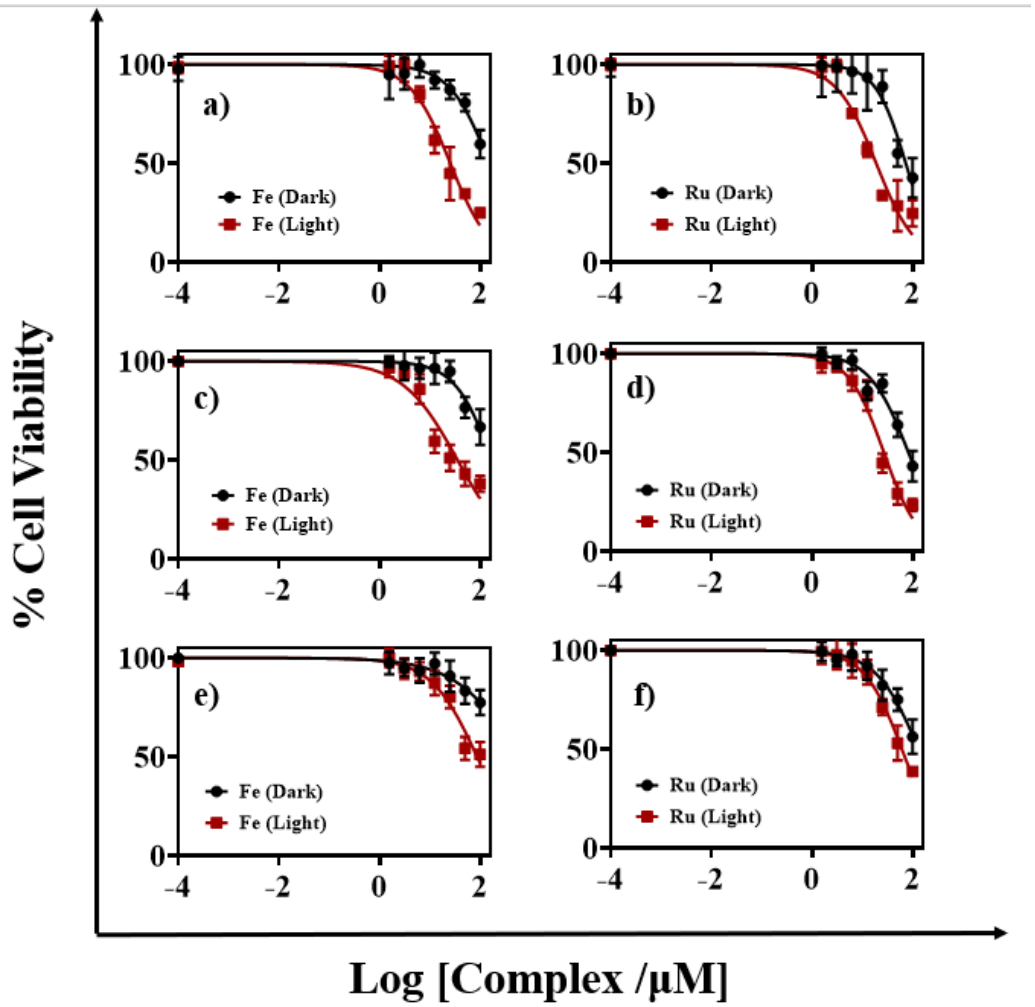

Figure S25. Cell viability (MTT assay) plots showing the cytotoxicity of **Fe** and **Ru** complex in A549 cells (a,b), HeLa cells (c,d), HPL1D cells (e,f) in the dark (black symbols) and in the presence of red light (red symbols, 600-720 nm, 30 J cm^{-2}).

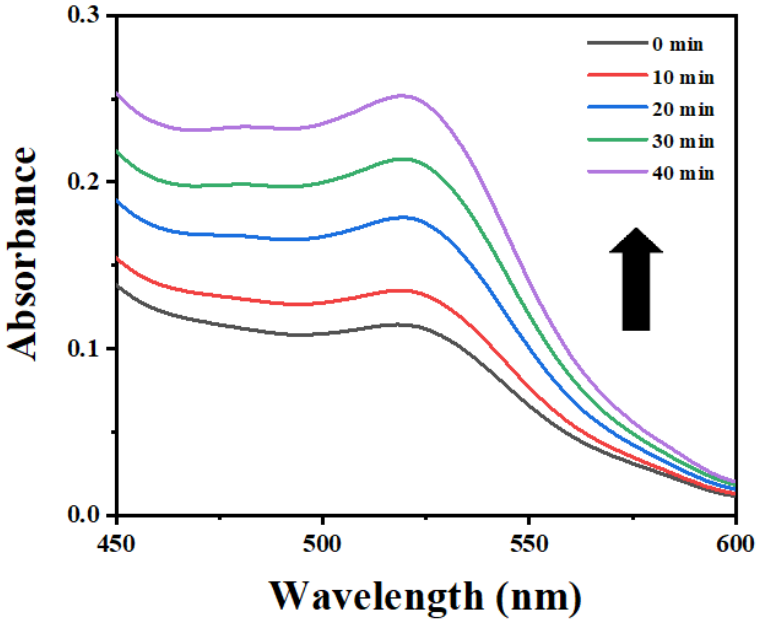

Figure S26. UV-visible spectrum traces showing the formation of hydroxyl radicals (•OH) on photo-activation of **Fe** (0.3 mM) with red light (600-720 nm, 30W, 0-30 min) in 5% DMSO-PBS buffer (pH 7.4) in the presence of benzoic acid. The enhancement in the absorbance at ~520 nm suggested the formation of Fe(III)-salicylate complex.

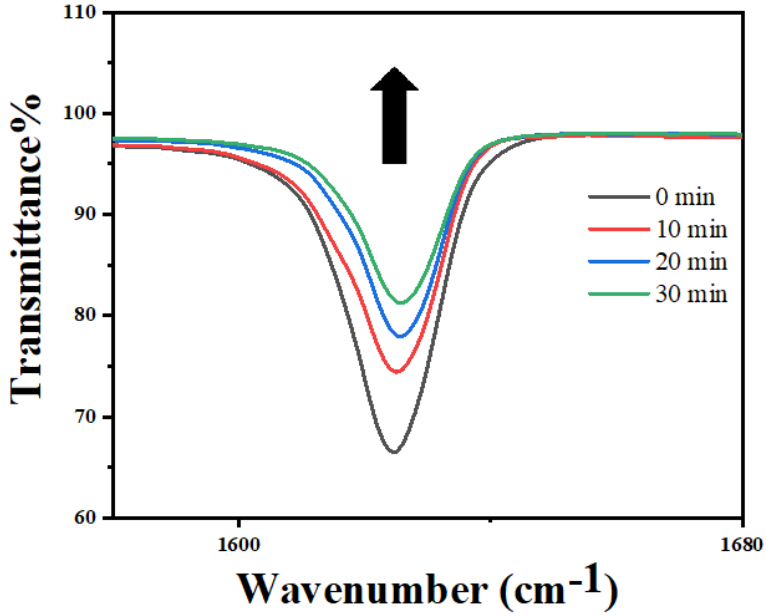

Figure S27. Photodecarboxylation of complex **Fe** through IR spectra traces show decrease in $C{=}O_{str}$ (COO of Fe-complex) upon illuminating **Fe** with red light (600-720 nm, 10 Jcm^{-2}, 0-30 min).

Table S28. Linear best fit plot table in DBPF assay examined with Rose Bengal (5 μM) (blue), [Fe-Ru] complex (0.2 mM) (black) and Ru-complex (0.2 mM) (red), relative to LED red light (30 W, 600–720 nm) in DMSO at 298 K.

Equation	y = a + b*x				
Plot	Complex	Complex	Ru complex	Rb	DPBF
Weight	No Weighting				
Intercept	0 ± --	0 ± --	0 ± --	0 ± --	0 ± --
Slope	0.00477 ± 1.96949E-5	0.00477 ± 1.96949E-5	0.003 ± 1.44117E-5	0.00649 ± 2.45426E-5	2.85462E-5 ± 2.65632E-6
Residual Sum of Squares	3.02553E-4	3.02553E-4	1.62004E-4	4.69825E-4	5.50371E-6
Pearson's r	0.9999	0.9999	0.99986	0.99991	0.95177
R-Square (COD)	0.9998	0.9998	0.99972	0.99983	0.90587
Adj. R-Square	0.99978	0.99978	0.9997	0.99981	0.89803

References

1. Pangborn, A.B.; Giardello, M.A.; Grubbs, R.H.; Rosen, R.K.; Timmers, F.J.Safe and Convenient Procedure for Solvent Purification, *Organometallics* **1995**, 15, 1518-1520.

2. Gazi, S.; Ananthakrishnan, R.; Semi-Quantitative Determination of Hydroxyl Radicals by Benzoic Acid Hydroxylation: An Analytical Methodology for Photo-Fenton Systems. *Curr. Anal. Chem.*, **2012,** 8, 143.

3. Musib, D.; Banerjee, S.; Garai, A.; Soraisam, U.; Roy, M.; Synthesis, Theory and In Vitro Photodynamic Activities of New Copper (II)-Histidinito Complexes. *Chemistry Select*., **2018**, 3, 2767-2775.

4. Pal, M.; Ramu, V.; Musib, D.; Kunwar, A.; Biswas, A.; Roy, M; Iron (III) Complex-Functionalized Gold Nanocomposite as a Strategic Tool for Targeted Photochemotherapy in Red Light, *Inorg. Chem.*, **2021**, 60, 6283-6297.

5. Wilson, J. J.; and Lippard, S. J.; In Vitro Anticancer Activity of cis-Diammineplatinum(II) Complexes with β-Diketonate Leaving Group Ligands, *J. Med. Chem.*, **2012**, 55, 5326-5336.

6. Shao, J.; Bao, W.G.; Tian, H.; Li, B.; Zhao, X. F.; Qiao, X.; Xu, J.Y.; Nuclease activity and protein-binding properties of a novel tetranuclear thiosemicarbazide Pt(II) complex. *Dalton Trans.*, **2014**, 43, 1663.

7. Skehan, P.; Storeng, R.; Scudiero, D.; Monks, A.; McMahon, J.; Vistica, D.; Warren, T.J.; Bokesch, H.; Kenney, S.; Boyd, R. M.; New colorimetric cytotoxicity assay for anticancer-drug screening. *J. Natl. Cancer Inst*., **1990**, 82, 1107-1112.

8. Raza, K.; Gautam, S.; Garai, A.; Mitra, K.; Kondaiah, P.; Chakravarty, A. R.; Monofunctional BODIPY-Appended Imidazoplatin for Cellular Imaging and Mitochondria-Targeted Photocytotoxicity. *Inorg. Chem.*, **2017**, 56, 11019-11029.

9. Elmes, R. B. P.; Orange, K. N.; Cloonan, S. M.; Williams, D. C.; Gunnlaugsson, T.; Luminescent Ruthenium(II) Polypyridyl Functionalized Gold Nanoparticles; Their DNA Binding Abilities and Application As Cellular Imaging Agents. *J. Am. Chem. Soc.*, **2011** 133, 15862–15865.

10. Musib, D.; Pal, M.; Raza, M. K.; Roy, M. Photo-physical, theoretical and photo-cytotoxic evaluation of a new class of lanthanide(iii)–curcumin/diketone complexes for PDT application. *Dalton Trans*., **2020**, 49, 10786-10798.

11. Peña, B.; Saha, S.; Barhoumi, R.; Burghardt, R. C.; Dunbar, K. R. Ruthenium(II)-Polypyridyl Compounds with π-Extended Nitrogen Donor Ligands Induce Apoptosis in Human Lung Adenocarcinoma (A549) Cells by Triggering Caspase-3/7 Pathway. *Inorg. Chem.*, **2018**, 57 (20), 12777–12786. https://doi.org/10.1021/acs.inorgchem.8b01988